

In-flight size classification of carbon nanotubes by gas phase electrophoresis

S H Kim and M R Zachariah¹

Nanoparticle-based Manufacturing and Metrology Laboratory, Departments of Mechanical Engineering, and Chemistry and Biochemistry, University of Maryland, College Park, MD 20742, USA

and

National Institute of Standards and Technology, Gaithersburg, MD 20899, USA

E-mail: mrz@umd.edu

Received 9 June 2005, in final form 19 July 2005

Published 9 August 2005

Online at stacks.iop.org/Nano/16/2149

Abstract

We demonstrate the use of gas phase electrophoresis to size classify CNTs grown in a continuous aerosol process. The separation process occurs at atmospheric pressure and involves electrostatic mobility separation which classifies fibres on the basis of equivalent projected surface area. This implies that one can, for diameter-controlled CNTs, obtain an on-the-fly determination of the CNT length distribution during CNT synthesis, or alternatively have a method for producing size separated CNTs. The method should be generic to any fibre based material.

Since the discovery of CNTs [1], many researchers have reported on the formation of diameter- and length-controlled CNTs grown on various substrates [2–6]. To produce diameter-controlled CNTs, uniform catalytic nanoparticle islands are employed, while the control of nanotube length is achieved by varying the time of exposure of catalyst particles to the carbon precursor and reducing gas mixtures [2–6].

In contrast gas phase synthesis of CNTs has the advantage of continuous production of CNTs [7–10]. However, unlike the well-defined growth conditions for substrate grown CNTs, the gas phase derived CNTs may have a range of ill-defined polydisperse diameters and lengths, resulting from the nature of the catalyst generation process [7–9] or generation of both metal and carbon precursors, as for example from laser ablation [10]. Subsequent coagulation and sintering of catalysts in the gas phase continuously transform the morphology and size during the growth process. This poses two major questions. (1) How can one control the diameter and length for gas phase grown CNTs?, (2) How can one measure in real time and continuously the size distribution of CNTs grown in a continuous flow system?

In this paper we address these issues by employing first gas phase electrophoresis to select the diameter of the CNT to be formed, and second an electrophoretic step to length select the CNT. The procedure can thus be used as either a preparatory

method, or, perhaps more usefully, as an on-the-fly method for determining the size distribution of CNTs grown in an arbitrary process.

For the CNT source we employ IR pulsed laser ablation (PLA) of a nickel target, to generate the catalyst particles. A flow of nitrogen was continuously swept past the target surface to carry away the nickel vapour, and cause rapid quenching and nucleation of nickel particles. The polydisperse metal particles are introduced to a differential mobility analyser or electrostatic classifier (EC). The EC is a standard tool in aerosol sizing, but is employed here in a preparatory method for delivering size-selected nickel particles [11, 12]. The EC shown in figure 1 consists of a negative high voltage cylindrical central rod and a grounded cylindrical housing. Clean dry nitrogen is supplied around the central electrode, and the annular flow of polydisperse aerosol is introduced from the top of the EC column. Some fraction of the aerosol is charged by a radioactive ionizing source (Po-210-Beta emitter), or by UV illumination. The charged aerosol fraction will drift under the action of the electric field and the retarding drag force, while simultaneously flowing with the carrier gas toward the bottom of the classifier. For a given applied voltage and flow rate, all positively charged particles with the same ion mobility will pass through the annular slot. We have previously shown that particles smaller than the mean free path of the gas are separated on the basis of the equivalent projected surface area [13–15]. Mono-area particles passing through the

¹ Author to whom any correspondence should be addressed.

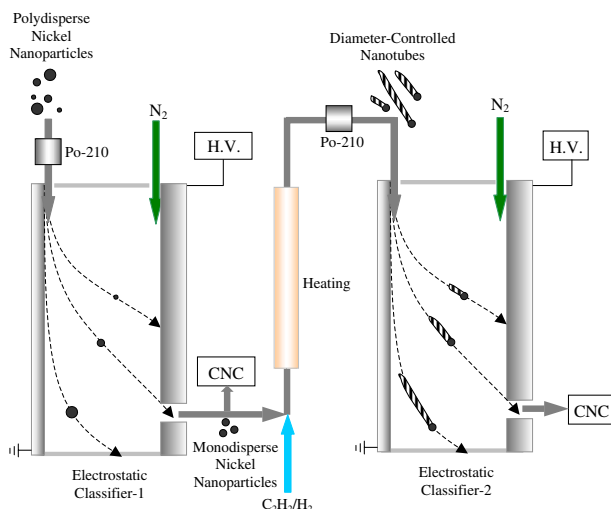


Figure 1. Schematic diagram of the length classification of nanotubes by gas phase electrophoresis using tandem mobility analysers. (H.V.: high voltage power supply, CNC: condensation nucleus counter).

(This figure is in colour only in the electronic version)

annular slot are detected by a condensation nucleus counter (CNC) [12, 16]. The size-selected nickel catalyst particles were sintered at the first tube furnace at 1200 °C, to form unagglomerated primary particles, from which CNTs were grown in free flight with the addition of acetylene (5 SCCM) and hydrogen (50 SCCM) at 750 °C, for a nominal growth time of ~5 s.

TEM images of Ni particles and CNTs are presented in figure 2. The Ni particles were fully sintered at 1200 °C (figure 2(a)), and the CNTs were grown on the size-selected Ni aerosol particles on-the-fly (figure 2(b)). Figure 2(c) presents the relative size distribution of the Ni aerosol particles and as-grown CNTs measured by tandem ECs and TEM analysis, respectively. The mean diameters of Ni particles and CNTs were $\sim 15 \pm 2$ nm and $\sim 14 \pm 2$ nm with the geometric mean standard deviation of 1.12 ± 0.02 and 1.15 ± 0.03 , respectively, indicating that the diameter of the CNTs is approximately equivalent to the diameter of the Ni aerosol particles.

The as-grown CNTs, which are nominally be of uniform diameter, were then passed through a Po-210 source to generate bipolar gas ions, to produce an equilibrium charge distribution on the diameter-controlled CNTs [16]. The CNT-laden flow was then passed to a second classifier (EC-2), and the resulting size distribution was measured by sweeping the classifier voltage and counting with the CNC. Figure 3 presents results for the number distribution as a function of size (i.e. size distribution) measured by EC-2, with and without addition of the carbon source. Without carbon addition we see a single narrow mode corresponding to the EC-1 selected ~15 nm nickel catalyst particles. Upon addition of acetylene, the 15 nm mode disappears and a broad distribution with a mean equivalent mobility diameter of 84 nm appears. Addition of acetylene/hydrogen alone in the absence of catalyst resulted in no counts in the CNC, implying that the growth was catalyst mediated. This implies that the broad size distribution reflects the behaviour of the CNTs in this electrostatic classifier.

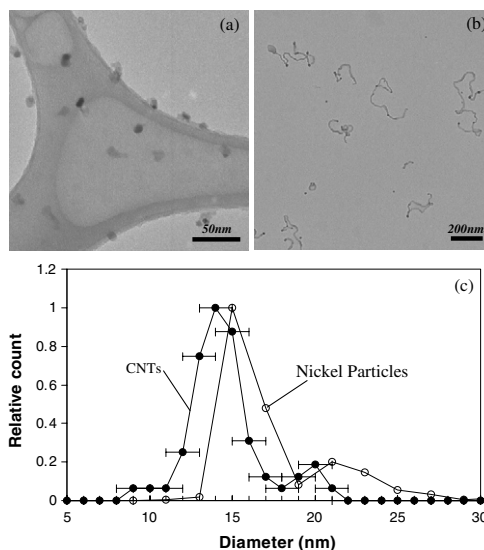


Figure 2. TEM images of (a) fully sintered Ni particles and (b) CNTs grown on the size-selected Ni particles, and the relative size distribution of Ni particles and CNTs measured by tandem electrostatic classifiers and TEM (digital image software), respectively.

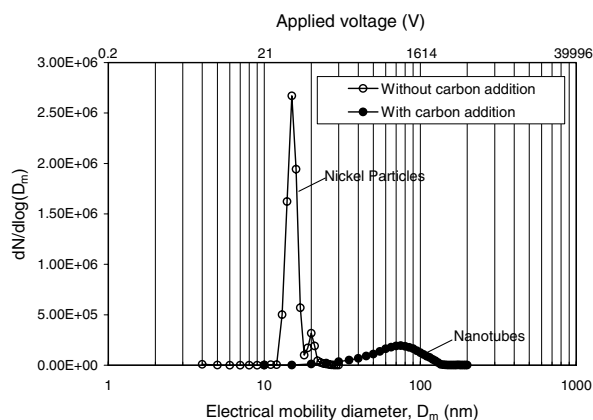


Figure 3. Number distribution of sintered size-selected nickel nanoparticles and nanotubes grown on the nickel nanoparticles as a function of electrical mobility diameter. (Experimental conditions: geometry of electrostatic classifier: $r_1 = 0.937$ cm (inner radius of electrode), $r_2 = 1.961$ cm (radius of housing), $L = 44.369$ cm (electrode length) and $Q_{sh} = 10$ lpm (sheath flow rate)).

Apparently then CNTs are segregated by a high electric field. We thus turn our attention to the nature of the classification and its utility.

The interpretation of the mobility distribution observed in figure 3 requires a consideration of how a cylindrical object might flow and orient in the electrostatic classifier. For a charged object, the separation mechanism is based on the number of charges on the object, and the charge location, and is known as electrophoresis. For an uncharged conducting object, the presence of a strong DC electric field may induce a dipole and result in migration, also known as dielectrophoresis. As a result, a dielectrophoresis separation mechanism would require that the nanotube be aligned parallel to the direction of the E -field as it flowed in the classifier, implying that the

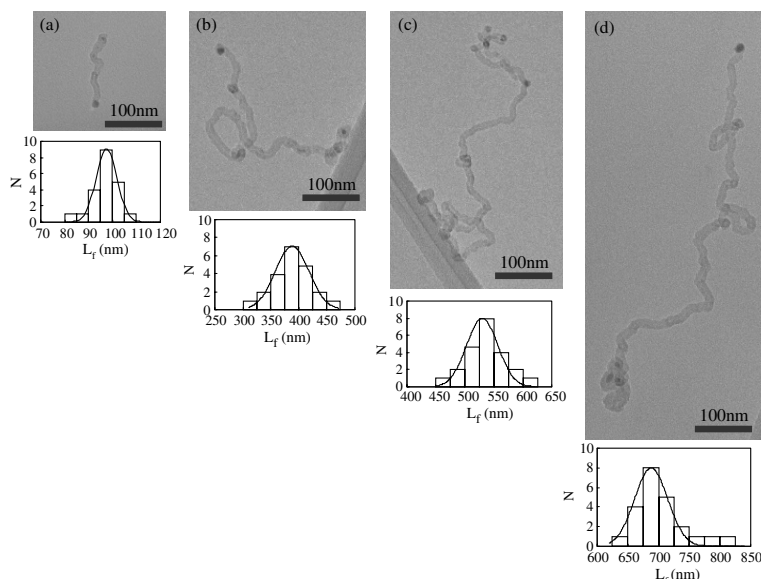


Figure 4. TEM images of uniform diameter nanotubes length-classified by gas phase electrophoresis at an equivalent electrical mobility diameter (applied voltage) of (a) $D_m = 50$ nm (465 V), (b) $D_m = 80$ nm (1089 V), (c) $D_m = 100$ nm (1607 V) and (d) $D_m = 120$ nm (2199 V) in the second electrostatic classifier.

dielectric force can suppress random Brownian tumbling of the nanotube.

To test the possibility of this mechanism we placed an electrostatic precipitator in line prior to EC-2 to remove any charged nanotubes, and found no signal counts as EC-2's voltage was swept. This implies that for the E -fields used to observe the distributions in figure 3, a dielectrophoresis mechanism is not operational, and that some type of electrophoretic mechanism is in play. It is reasonable to expect that the charge on the nanotube is at one of the ends of the tube. If so, then in the absence of Brownian motion the nanotube will align in the field so that it presents the smallest drag as it slips radially across the annular region. However, the nanotube also experiences a random and fluctuating torque, which we might consider as the Brownian rotational diffusion, and may perturb the alignment of the nanotube from being parallel to the electric field. By evaluating the integral of the torque over some angular displacement away from the parallel electric field direction, we can evaluate whether the ambient thermal energy is sufficient to disorient the CNT. We find for a singly charged nanotube with a diameter of 15 nm, and any length shorter than 2000 nm, that the Brownian thermal energy is sufficient to result in free rotational motion for fields up to ~ 3 kV cm $^{-1}$ [17]. A freely tumbling nanotube will present a drag force proportional to its projected surface area. And for diameter-selected nanotubes this implies that the electrophoretic separation must be a strong function of the nanotube length.

To verify our conceptual model, four different mobility sizes coming from EC-2 were deposited on TEM grids. Figure 4 shows the TEM images of as-classified nanotubes with different EC-2 applied voltages. From the images we observed that all the CNTs have uniform diameter of ~ 15 nm, reflecting the use of uniform sized metal catalytic particles coming from EC-1, and are also in agreement with the nickel size distribution shown in figure 2. The nanotubes formed were MWCNTs

with irregular alignment. Each micrograph containing many tens of nanotubes was processed to obtain the projected area of the nanotube using digital image processing software [18]. For a fixed diameter tube this allowed us to evaluate the total length of each tube. To minimize the error associated with the projection of a 3D object on a 2D plane, we excluded from our data analysis those CNTs showing significant morphological change when the TEM grid was tilted (up to 45°). This resulted in discarding approximately 10% of the images, which were of tubes that were either sitting off the surface at an angle or were significantly bent. The results for length are presented in figure 4 as histograms of number count (N) as a function of nanotube length (L_f) for each applied voltage of 465 V ($D_m = 50$ nm), 1089 V (80 nm), 1607 V (100 nm) and 2199 V (120 nm). The numbers in parenthesis indicate an equivalent mobility diameter, or an electrical mobility corresponding to a spherical particle of that diameter. For these voltages on EC-2, the as-classified nanotubes had an average length of 127 ± 13 nm, 370 ± 37 nm, 603 ± 61 nm, 891 ± 90 nm, respectively. The length of classified nanotubes increases with increasing applied voltage, and indicates that gas phase electrophoresis can separate nanotubes on the basis of length.

However, more relevant perhaps is how to interpret the applied voltage, corresponding to a mobility size, as a measure of the CNT length distribution directly. To do this we extract the nanotube length distribution on the basis of the nanotube mobility size distribution, by using the digital image software to find the relation between projected area diameter (D_A) of the as-classified nanotubes, and the electrical mobility diameter. If the nanotube is indeed tumbling in an electric field, the processed mobility diameter (D_m) should correspond to the projected area diameter. Figure 5 shows a plot of the projected area diameter determined from the TEM images versus the electrical mobility diameter extracted from EC-2. We observe a deviation of less than 10%. This indicates that diameter-controlled CNTs with the same electrical mobility have a

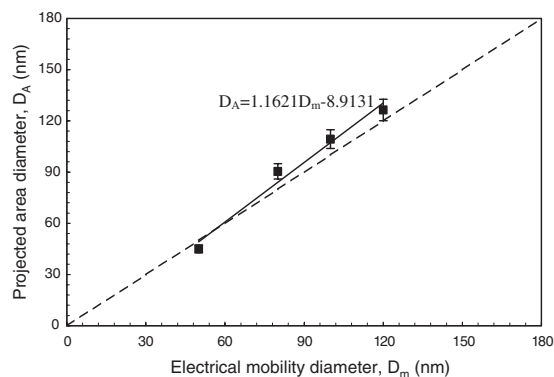


Figure 5. Comparison of the projected area diameter of nanotubes (from TEM) with the electrical mobility diameter (from electrophoretic separation). The dotted line is for $D_A = D_m$.

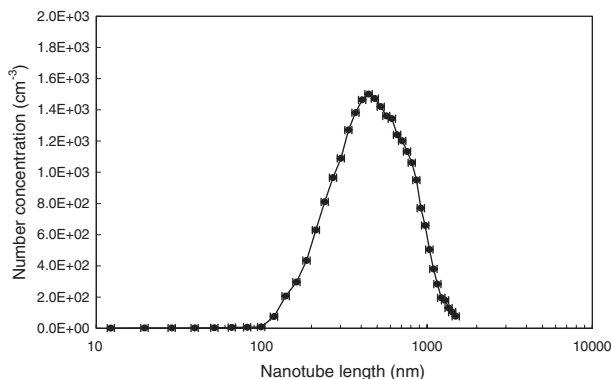


Figure 6. Length distribution of nanotubes classified by the electrostatic classifier.

uniform length, regardless of their shape. However, we believe that the deviation between D_A and D_m for CNTs may be greater for longer chains than for agglomerates, due to alignment in the E -field. At the higher fields necessary for extracting longer tubes, the thermal energy necessary to randomize the chains becomes too large and the field can finally align the tube. This will result in an effective decrease in the apparent drag force and make the mobility diameter seem smaller than the projected area diameter that we measure by TEM. We believe that the deviation seen in figure 5 is just this effect and will increase with increasing length.

On the basis of the relation between D_A and D_m found in figure 5 ($D_A = C_1 \cdot D_m + C_2$, where $C_1 = 1.1621$, $C_2 = -8.9131$), we work back to calculate the length distribution of nanotubes on the basis of the mobility size distribution curve shown in figure 3. Since we have uniform diameter nanotubes in all electrical mobility size ranges, the length of nanotubes was calculated from $L_f = (\pi/4D_f)[(D_A - C_2)/C_1]^2$, where L_f is the CNT length, D_f is the CNT diameter and D_A is the projected area diameter.

Figure 6 shows the number distribution as a function of nanotube length calculated using the above equation, and the mobility distribution given in figure 3. The number mean length of CNTs is 450 nm, with a geometric standard deviation (GSD) of 1.66. The relatively large GSD implies that for our particular experimental growth conditions not all catalysts were equally active. This illustrates that the method could be used as an on-the-fly process measurement tool for CNT growth, and a direct method for either length classifying, or providing a nanotube size distribution measurement, on the basis of gas phase electrophoresis. The method should be even more accurate for SWCNTs, and should be generically applicable to any nanostructure with a high aspect ratio.

Methods

The catalyst particle chosen for CNT growth in this approach was nickel, which was generated by pulsed laser ablation of a solid nickel target, using a 1064 nm Q-switched Nd:YAG laser operating at 10 Hz with a pulse width of 4 ns. The laser

beam is focused through a fused silica plano-convex lens (focal length = 100 mm) to a spot on the solid nickel target, with an approximate laser fluence of $\sim 10^{10}$ W cm $^{-2}$ at the focal point. This generates a local microplasma at the surface of the nickel target, leading to vaporization. The nickel target was mounted on a rotating shaft with a stepper motor, so that the target could be rotated with a controlled interval to provide long term stability in the particle generation process.

References

- [1] Iijima S 1991 *Nature* **354** 56
- [2] Andrews R, Jacques D, Rao A M, Rantell T, Derbyshire F, Chen Y, Chen J and Haddon R C 1999 *Appl. Phys. Lett.* **75** 1329
- [3] Rueckes T, Kim K, Joselevich E, Tseng G Y, Cheung C-L and Lieber C M 2000 *Science* **289** 94
- [4] Ren Z F, Huang Z P, Xu J W, Wang J H, Bush P, Siegel M P and Provencio P N 1998 *Science* **282** 1105
- [5] Hata K, Futaba D N, Mizuno K, Namai T, Yumura M and Iijima S 2004 *Science* **306** 1363
- [6] Cheung C L, Kurtz A, Park H and Lieber C M 2002 *J. Phys. Chem. B* **106** 2429
- [7] Bronikowski M J, Willis P A, Colbert D T, Smith K A and Smalley R E 2001 *J. Vac. Sci. Technol. A* **19** 1800
- [8] Ci L, Li Y, Wei B, Liang J, Xu C and Wu D 2000 *Carbon* **38** 1933
- [9] Ago H, Ohshima S, Uchida K and Yumura M 2001 *J. Phys. Chem. B* **105** 10453
- [10] Yudasaka M, Ichihashi T, Komatsu T and Iijima S 1999 *Chem. Phys. Lett.* **299** 91
- [11] Higgins K, Jung H, Kittelson D B, Roberts J T and Zachariah M R 2002 *J. Phys. Chem. A* **106** 96
- [12] Knutson E O and Whitby K T 1975 *J. Aerosol Sci.* **6** 443
- [13] Rogak S N, Flagan R C and Nguyen H V 1993 *Aerosol Sci. Technol.* **18** 25
- [14] Jung H, Kittelson D B and Zachariah M R 2004 *Combust. Flame* **136** 445
- [15] Park K, Kittelson D B, Zachariah M R and McMurry P H 2004 *J. Nanopart. Res.* **6** 267
- [16] Kim S H, Woo K S, Liu B Y H and Zachariah M R 2005 *J. Colloid Interface Sci.* **282** 46
- [17] Lilienfeld P 1985 *J. Aerosol Sci.* **16** 315
- [18] Image J, National Institutes of Health <http://rsb.info.nih.gov/nih-image/>